

An Explicit-Implicit Mixed Staggered Asynchronous Step Integration Algorithm in Structural Dynamics

Zhiqiang Ma^{1,2}, Lingshuang Kong^{1,2} and Xianlong Jin^{1,2,*}

Abstract: Many engineering applications need to analyse the system dynamics on the macro and micro level, which results in a larger computational effort. An explicit-implicit asynchronous step algorithm is introduced to solve the structural dynamics in multi-scale both the space domain and time domain. The discrete FEA model is partitioned into explicit and implicit parts using the nodal partition method. Multiple boundary node method is adopted to handle the interface coupled problem. In coupled region, the implicit Newmark coupled with an explicit predictor corrector Newmark whose predictive wave propagates into the implicit mesh. During the explicit subcycling process, the variables of boundary nodes are solved directly by dynamics equilibrium equation. The dissipation energy is dynamically determined in accordance with the energy balance checking. A cantilever beam and a building two numerical examples are proposed to verify that the method can greatly reduce the computing time while maintaining a high accuracy.

Keywords: Structural dynamics, node partition, Newmark method, explicit-implicit asynchronous integration, stability condition

1 Introduction

Explicit and implicit time integration algorithms are the two direct integration algorithms in the transient dynamic analysis.

With the improvement of numerical simulation method, there is a growing demand to solve dynamic problems with different temporal and spatial scale. The explicit and implicit algorithms are often combined to solve the problem, in order to take advantage of different algorithms [Hughes (2012)]. There are two kinds of combination approach, one is explicit and implicit algorithms used sequentially to solve the problem in the time domain, the other is to use different family algorithm in different spatial domain.

In the first case, a reasonable approach is to integrate explicit and implicit algorithms into a unified program. The algorithm shift from one family to another according to the appropriate transition condition. It is necessary to deal with the numerical oscillation of explicit and implicit switching [Jung and Yang (1998)]. This kind of method is used to

¹ State Key Laboratory of Mechanical System and Vibration, Shanghai Jiao Tong University, No. 800 Dongchuan Road, Shanghai, 200240, China.

² School of Mechanical Engineering, Shanghai Jiao Tong University, No. 800 Dongchuan Road, Shanghai 200240, China.

* Corresponding Author: Xianlong Jin. Email: jxlong@sjtu.edu.cn.

predict springback in sheet metal forming by Narkeeran and Lovell [Narasimhan and Lovell (1999)]. Noels used this explicit-implicit combined method to handle crashworthiness analysis [Noels, Stainier and Ponthot (2004); Noels (2006)]. Bock presented a unified framework for the numerical solution of optimal control problems solved with both implicit and explicit switches [Bock, Kirches and Meyer (2018)].

For another type of combination, the element partition and nodal partition are applied. The structure is divided into a number of subdomains. Each subdomain has its own integration scheme and time step. This kind of research originates from Belytschko and Hughes [Belytschko and Mullen (1978); Hughes and Liu (1978)]. In the later decades, many representative algorithms have emerged. The algorithms can be divided into two categories: with or without overlapping region.

In the context of non-overlapping subdomain coupling method, Schur-type approaches and dual Schur-type approaches are two typical methods. The Schur-type method enforces the displacement or acceleration continuity at the interface [Mahjoubi, Gravouil and Combescure (2009)]. Liu et al. [Liu and Belytschko (1982)] developed a new family of implicit-explicit algorithm which permits different time integration and different time steps to be used simultaneously by element partitioning. Smolinski et al. [Smolinski, Belytschko and Neal (1988); Wu and Smolinski (2000)]. Daniel proposed an implicit subcycling algorithm [Daniel (2003)] developed an explicit subcycling algorithm by nodal partitioning.

For dual Schur-type approaches, Gravouil et al. [Gravouil and Combescure (2002)] proposed a multi-time-step dual Schur approach with a velocity continuity condition on the interface at the fine time step, which referenced as GC method. Prakash et al. [Prakash and Hjelmstad (2004)] developed the PH method which enforced continuity of velocity at the coarse time step but only valid for two subdomains. Karimi et al. [Karimi and Nakshatrala (2014)] compared the GC method and PH method in detail and a new multi-time-step monolithic coupling method combining the advantages of both methods is developed.

For overlapping subdomain coupling method, The Arlequin framework is a representative method [Ghanem, Torkhani, Mahjoubi et al. (2013)]. In recent years, explicit-implicit mixed method is gradually combined with adaptive time step or improve the performance and application scope of the algorithm [Soares (2018); Fernandes, Cardoso and Mansur (2017)]. Fekak extended the explicit-implicit method to the field of nonsmooth dynamics [Fekak, Brun, Gravouil et al. (2017)]. Dimarco developed a high order implicit-explicit linear multistep methods for kinetic equations [Dimarco and Pareschi (2017)]. In simulation of three-dimensional grapheme, a hybrid implicit-explicit finite-difference time-domain method is presented [Chen and Wang (2016)].

When mixed with different time steps, the assumption of linear acceleration or linear velocity is applied to tackle the partition boundary conditions. The interpolation process of Lagrange multipliers is used to deal the interface problem. This approach is often regarded as the source of error accumulation and the development of instability, which has led to a bigger error of the calculation result and a harsh condition [Biesiadecki and Skeel (1993)].

In this article, we use the dynamic multiple boundary method to handle the explicit and implicit boundary information transmission. The variable of the boundary nodes is solved

directly by explicit transfer process. Numerical cases show that our modification results in a higher accuracy than classical interpolation method. The proposed method can increase computational efficiency by using nodal partition and asynchronous time step method.

The rest of this paper is organized as follows: In Section 2, the Newmark integrator and explicit Newmark based on predictor-corrector formula schemes are introduced to solve the structural dynamic equation. Then, In Section 3 The asynchronous explicit-implicit integration process is proposed to use different time scales and integral methods in different regions. In Section 4, The check of energy balance for the explicit-implicit mixed asynchronous step method is described. In Section 5, two numerical examples are conducted to verify the rationality and feasibility of the explicit-implicit mixed asynchronous method. Finally, conclusions are drawn in Section 6.

2 The Newmark discretized solution procedure

The finite element discretized of a structure which leads to the semi-discretized dynamic equilibrium equation can be written as Cook [Cook (2007)].

$$\mathbf{M}\mathbf{a}(t) + \mathbf{C}\mathbf{v}(t) + \mathbf{f}^{int}(\mathbf{u}(t)) = \mathbf{f}^{ext}(t) \quad (1)$$

Where \mathbf{M} is the mass matrix, \mathbf{a} is the nodal acceleration vector, \mathbf{C} is the damping matrix, \mathbf{f}^{int} and \mathbf{f}^{ext} are the vectors of internal and external force respectively. The given initial displacement and velocity conditions is $\mathbf{u}(t_0)=\mathbf{u}_0$ and $\mathbf{v}(t_0)=\mathbf{v}_0$. For linear elasticity, the equilibrium equation is a second-order time differential equation and the internal force vector \mathbf{f}^{int} can be written as

$$\mathbf{f}^{int}(\mathbf{u}(t)) = \mathbf{K}\mathbf{u}(t) \quad (2)$$

Where \mathbf{K} is the symmetric stiffness matrix, \mathbf{v} and \mathbf{u} are the nodal velocity and displacement vectors. The Eq. (1) can be solved by discretized in time among which the Newmark based time integrator is mostly used.

2.1 The Newmark integrator scheme

The Newmark method has two parameters γ and β . Displacement, velocity and acceleration vectors of generalized structural nodes from time t_n to time t_{n+1} are based on the equilibrium of the dynamic equation [Cook (2007)]. Subscript n is used to denote the time step. At the time step t_{n+1}

$$\begin{aligned} \mathbf{u}_{n+1} &= \mathbf{u}_n + \mathbf{v}_n \Delta t + \left(\frac{1}{2} - \beta\right) \mathbf{a}_n \Delta t^2 + \beta \mathbf{a}_{n+1} \Delta t^2 \\ \mathbf{v}_{n+1} &= \mathbf{v}_n + (1 - \gamma) \mathbf{a}_n \Delta t + \gamma \mathbf{a}_{n+1} \Delta t \end{aligned} \quad (3)$$

\mathbf{u}_{n+1} , \mathbf{v}_{n+1} , \mathbf{a}_{n+1} are the displacement, velocity and acceleration vectors at time step $n+1$ respectively. \mathbf{u}_n , \mathbf{v}_n , \mathbf{a}_n are the displacement, velocity and acceleration vectors at time step n . Δt is the time step. In the Newmark integral method, the displacement \mathbf{u}_{n+1} in time t_{n+1} is solved from the dynamic equation

$$\begin{aligned} & \left(\mathbf{K} + \frac{1}{\beta\Delta t^2} \mathbf{M} + \frac{\gamma}{\beta\Delta t} \mathbf{C} \right) \mathbf{u}_{n+1} = \mathbf{f}_{n+1} + \mathbf{M} \left[\frac{1}{\beta\Delta t^2} \mathbf{u}_n + \frac{1}{\beta\Delta t} \mathbf{v}_n + \left(\frac{1}{2\beta} - 1 \right) \mathbf{a}_n \right] + \\ & \mathbf{C} \left[\frac{\gamma}{\beta\Delta t} \mathbf{u}_n + \left(\frac{\gamma}{\beta} - 1 \right) \mathbf{v}_n + \left(\frac{\gamma}{2\beta} - 1 \right) \Delta t \mathbf{a}_n \right] \end{aligned} \quad (4)$$

The above equation can be rewritten as

$$\mathbf{K}_{eff} \mathbf{u}_{n+1} = \bar{\mathbf{f}}_{n+1} \quad (5)$$

The matrix \mathbf{K}_{eff} in the above equation is referred as the effective stiffness matrix. The matrix \mathbf{K}_{eff} and external force vector $\bar{\mathbf{f}}_{n+1}$ are defined as

$$\begin{aligned} \mathbf{K}_{eff} &= \mathbf{K} + \frac{1}{\beta\Delta t^2} \mathbf{M} + \frac{\gamma}{\beta\Delta t} \mathbf{C} \\ \bar{\mathbf{f}}_{n+1} &= \mathbf{f}_{n+1} + \mathbf{M} \left[\frac{1}{\beta\Delta t^2} \mathbf{u}_n + \frac{1}{\beta\Delta t} \mathbf{v}_n + \left(\frac{1}{2\beta} - 1 \right) \mathbf{a}_n \right] + \mathbf{C} \left[\frac{\gamma}{\beta\Delta t} \mathbf{u}_n + \left(\frac{\gamma}{\beta} - 1 \right) \mathbf{v}_n + \left(\frac{\gamma}{2\beta} - 1 \right) \Delta t \mathbf{a}_n \right] \end{aligned} \quad (6)$$

In all time steps the effective stiffness matrix \mathbf{K}_{eff} remains constant in linear dynamic analysis.

2.2 The explicit newmark based on predictor-corrector scheme

In the predictor-corrector time discretion of explicit Newmark scheme, the predictors of the scheme can be written as Hughes [Hughes (2012)]

$$\begin{aligned} \mathbf{u}_{n+1}^p &= \mathbf{u}_n + \mathbf{v}_n \Delta t + \left(\frac{1}{2} - \beta \right) \mathbf{a}_n \Delta t^2 \\ \mathbf{v}_{n+1}^p &= \mathbf{v}_n + \Delta t (1 - \gamma) \mathbf{a}_n \end{aligned} \quad (7)$$

The vectors \mathbf{u}_{n+1}^p and \mathbf{v}_{n+1}^p means the corresponding predictor displacement and velocity vectors at time step $n+1$. The predictor form of the structural dynamic equation can be defined as

$$\mathbf{M} \mathbf{a}_{n+1} + \mathbf{C} \mathbf{v}_{n+1}^p + \mathbf{K} \mathbf{u}_{n+1}^p = \mathbf{f}_{n+1} \quad (8)$$

If the lumped mass matrix is adopted, the mass matrix \mathbf{M} is diagonal and the method is explicit. The nodal acceleration vector \mathbf{a}_{n+1} can be solved from the dynamic equation

$$\mathbf{a}_{n+1} = \mathbf{M}^{-1} (\mathbf{f}_{n+1} - \mathbf{C} \mathbf{v}_{n+1}^p - \mathbf{K} \mathbf{u}_{n+1}^p) \quad (9)$$

Then, the corrector displacement \mathbf{u}_{n+1} and velocity \mathbf{v}_{n+1} vectors of $n+1$ time step can be obtained from the equations

$$\begin{aligned} \mathbf{u}_{n+1} &= \mathbf{u}_{n+1}^p + \beta \Delta t^2 \mathbf{a}_{n+1} \\ \mathbf{v}_{n+1} &= \mathbf{v}_{n+1}^p + \gamma \Delta t \mathbf{a}_{n+1} \end{aligned} \quad (10)$$

With the provided initial displacement \mathbf{u}_0 and velocity \mathbf{v}_0 conditions, the initial acceleration \mathbf{a}_0 can be solved as follows

$$\mathbf{a}_0 = \mathbf{M}^{-1} (\mathbf{f}_0 - \mathbf{C} \mathbf{v}_0 - \mathbf{K} \mathbf{u}_0) \quad (11)$$

3 The explicit-implicit coupling method with overlapping node

3.1 Notation and tag for explicit-implicit coupling

There are two partition methods, namely mesh partition and node partition. The overlapping node partition method is used. The elements fall into three groups: Explicit region, implicit region and interface elements. The schematic of node partition with overlapping node is shown in Fig. 1.

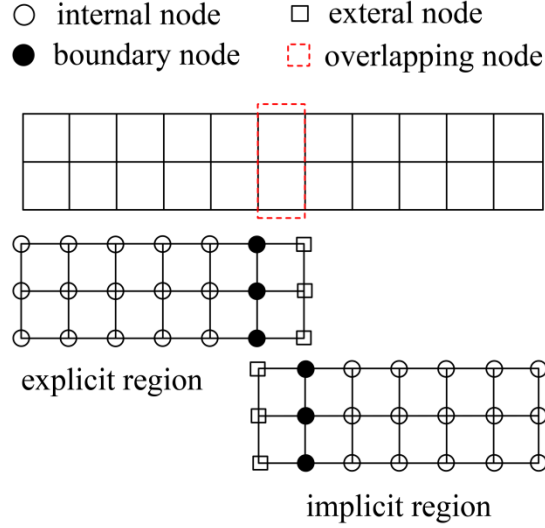


Figure 1: Node partition diagram with overlapping node

For each subdomain, the nodes can be divided into internal node, external node and boundary node. The displacement for explicit subdomain can be described as $\mathbf{u}_I^E, \mathbf{u}_B^E$ and \mathbf{u}_E^E . The superscript letter E represents the explicit partition and the subscript represents the node type. The displacement for implicit subdomain can be described as $\mathbf{u}_I^I, \mathbf{u}_B^I$ and \mathbf{u}_E^I . The external node in explicit subdomain is the boundary node in implicit subdomain and vice versa.

We define the tags $\mathbf{u}^E = [\mathbf{u}_I^E \ \mathbf{u}_B^E]^T$ and $\mathbf{u}^I = [\mathbf{u}_I^I \ \mathbf{u}_B^I]^T$ to represent the non-overlapping subdomain nodal displacement. The superscripts E and I represent the explicit and implicit region. Velocity, acceleration and external force vectors have the same tags.

The time step for the explicit region Δt_r can be defined as

$$\Delta t_r = \alpha \min(\Delta t_{cr}^i) \quad (i = 1, 2, \dots, nelem) \quad (12)$$

Δt_{cr}^i is the critical time step for element i confirmed by the CFL condition. α is the scale factor. A larger time step Δt is adopted to implicit region. The time step ratio m between explicit and implicit region can be defined as

$$m := \frac{\Delta t}{\Delta t_r} \quad (m \in N^*) \quad (13)$$

The following notation represents the value of a quantity at subdomain time level. \mathbf{X} indicates displacement, velocity or acceleration

$$\mathbf{X}_{n+j/m}^i := \mathbf{X}^i(t = n\Delta t_i + j\Delta t_r) \quad (j \leq m) \tag{14}$$

n is the number for system time step and j is for subcycling time step. The asynchronous time step in system time level is shown in Fig. 2

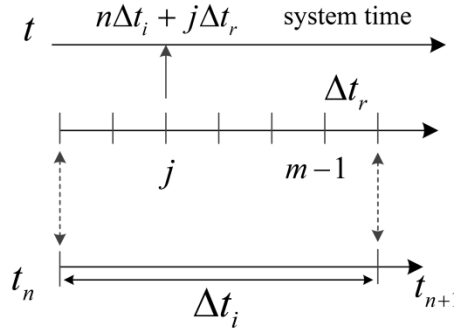


Figure 2: Suddomain and system time step

3.2 The asynchronous step explicit-implicit integration coupling method

The time steps for implicit and explicit region are Δt and Δt_r . The step ratio satisfies $\Delta t = m\Delta t_r$. The multi-layer boundary node method is used to tackle the asynchronous step explicit-implicit coupling algorithm. Multi-layer overlapping node consists boundary node and external node. In order to explain the method clearly, we take the step ratio $m=3$ for example. Data matching for multi overlapping node is shown in Fig. 3.

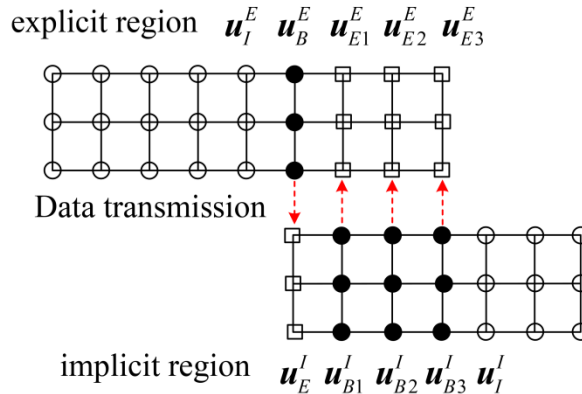


Figure 3: Data matching for multi overlapping node

For explicit region, the nodal displacement is defined as $u_I^E, u_B^E, u_{E1}^E, u_{E2}^E$ and u_{E3}^E . $u_E^I, u_{B1}^I, u_{B2}^I, u_{B3}^I$ and u_I^I are displacement tags for implicit region.

The equilibrium equation of the linear structural dynamics at time step n can be partitioned as

$$\begin{bmatrix} \mathbf{M}^E & 0 \\ 0 & \mathbf{M}^I \end{bmatrix} \begin{Bmatrix} \mathbf{a}_n^E \\ \mathbf{a}_n^I \end{Bmatrix} + \begin{bmatrix} \mathbf{C}^E & \mathbf{C}^{EI} \\ \mathbf{C}^{IE} & \mathbf{C}^I \end{bmatrix} \begin{Bmatrix} \mathbf{v}_n^E \\ \mathbf{v}_n^I \end{Bmatrix} + \begin{bmatrix} \mathbf{K}^E & \mathbf{K}^{EI} \\ \mathbf{K}^{IE} & \mathbf{K}^I \end{bmatrix} \begin{Bmatrix} \mathbf{u}_n^E \\ \mathbf{u}_n^I \end{Bmatrix} = \begin{Bmatrix} \mathbf{f}_n^E \\ \mathbf{f}_n^I \end{Bmatrix} \quad (15)$$

The damping matrix \mathbf{C} is assumed in the form of Rayleigh damping. While different from the Belytschko method [Belytschko and Mullen (1978)], the predictor corrector form explicit Newmark scheme is used to solve the nodal acceleration of explicit region. During the explicit subcycling process, the explicit region need to be updated all nodes through time step $m-1$

$$\begin{aligned} (\mathbf{u}_{n+j/m}^E)^p &= \mathbf{u}_{n+(j-1)/m} + \mathbf{v}_{n+(j-1)/m} \Delta t_r + \left(\frac{1}{2} - \beta\right) \mathbf{a}_{n+(j-1)/m} \Delta t_r^2 \\ (\mathbf{v}_{n+j/m}^E)^p &= \mathbf{v}_{n+(j-1)/m} + (1 - \gamma) \mathbf{a}_{n+(j-1)/m} \Delta t_r \end{aligned} \quad (16)$$

The supermark E represents all explicit nodes. The nodal acceleration of explicit region can be solved as

$$\mathbf{a}_{n+j/m}^E = (\mathbf{M}^E)^{-1} [\mathbf{f}_{n+j/m}^E - \mathbf{C}^E (\mathbf{v}_{n+j/m}^E)^p - \mathbf{K}^E (\mathbf{u}_{n+j/m}^E)^p - \mathbf{C}_{BE}^E (\mathbf{v}_{E,n+j/m}^E)^p - \mathbf{K}_{BE}^E (\mathbf{u}_{E,n+j/m}^E)^p] \quad (17)$$

Where $j=1, 2, 3 \dots m$.

The displacement and velocity of the explicit non-overlapping nodes are corrected by the Eq. (10). The displacement of implicit region is calculated after explicit subdomain. The expression is as follows

$$\mathbf{K}_{eff}^I \mathbf{u}_{n+1}^I = \bar{\mathbf{f}}_{n+1}^I \quad (18)$$

Where $\mathbf{K}_{eff}^I = (\mathbf{K}^I + \frac{1}{\beta \Delta t^2} \mathbf{M}^I + \frac{\gamma}{\beta \Delta t} \mathbf{C}^I)$ is the effective stiffness matrix. The effective external force $\bar{\mathbf{f}}_{n+1}^I$ is defined as

$$\bar{\mathbf{f}}_{n+1}^I = \mathbf{f}_{n+1}^I + \frac{\mathbf{M}^I}{\beta \Delta t^2} (\mathbf{u}_{n+1}^I)^p - \mathbf{C}^I (\mathbf{v}_{n+1}^I)^p + \frac{\gamma}{\beta \Delta t} \mathbf{C}^I (\mathbf{u}_{n+1}^I)^p - \mathbf{K}_{EB}^I \mathbf{u}_{E,n+1}^I - \mathbf{C}_{EB}^I \mathbf{v}_{E,n+1}^I$$

The subscript $n+1$ means system time $(n+1)\Delta t = n\Delta t + m\Delta t_r$. The acceleration \mathbf{a}_{n+1}^I and velocity \mathbf{v}_{n+1}^I vectors of the implicit region are defined as

$$\begin{cases} \mathbf{a}_{n+1}^I = (\mathbf{u}_{n+1}^I - (\mathbf{u}_{n+1}^I)^p) / \beta m^2 \Delta t^2 \\ \mathbf{v}_{n+1}^I = (\mathbf{v}_{n+1}^I)^p + \gamma (\mathbf{u}_{n+1}^I - (\mathbf{u}_{n+1}^I)^p) / \beta m \Delta t \end{cases} \quad (19)$$

With the increase of explicit subcycling time step, the external node which can be solved correctly in explicit region is decrease. The internal and boundary nodes for explicit region can be solved correctly during the subcycling time step. Before the next system step, external nodes need data transmission as $\mathbf{u}_E^I = \mathbf{u}_B^E$ and $\mathbf{u}_{Ei}^E = \mathbf{u}_{Bi}^I$ ($i=1, 2 \dots m$).

The two-dimensional nodal time-displacement flow of the asynchronous explicit-implicit method is shown in Fig. 4.

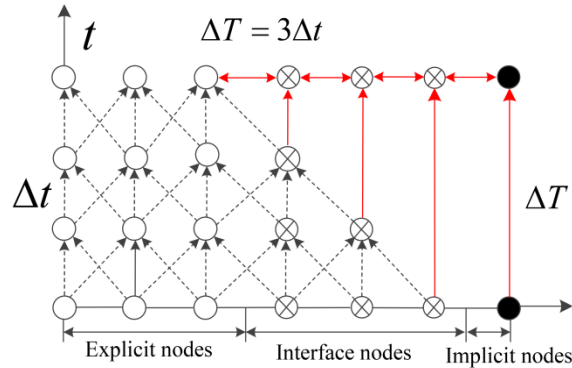


Figure 4: Message passing for asynchronous time step calculation

The proposed method uses the equilibrium equation to solve the acceleration of the boundary node which completely preserves the precision of boundary node.

4 Energy balance check for numerical stability

In the compute process, any unstable result can lead to pseudo energy. By checking the energy balance, the calculation of stability can be checked in real time. For the linear without structural damping case, the system internal energy w^{int} , work of the external force w^{ext} and kinetic energy w^{kin} are defined as Krenk [Krenk (2006)]

$$\begin{aligned} W^{int} &= \frac{1}{2} \mathbf{u}^T \mathbf{K} \mathbf{u} \\ W^{ext} &= \mathbf{u}^T \mathbf{f}^{ext} \\ W^{kin} &= \frac{1}{2} \mathbf{v}^T \mathbf{M} \mathbf{v} \end{aligned} \quad (20)$$

According to the principle of energy conservation, the energy requirements in the processes of solving the dynamic equation have the following equation

$$W_n^{dis} = \left| W_n^{kin} + W_n^{int} - W_n^{ext} \right| \leq \varepsilon \max(W^{kin}, W^{int}, W^{ext}) \quad (21)$$

ε is a very small error tolerance limit whose general order of magnitude is 10^{-2} . The energy balance calculation can be implemented in each sub region if the overall dynamic system is very large.

5 Numerical examples and discussion

In the following two examples, we assume the parameters of implicit scheme $\gamma^I = 0.5$ and $\beta^I = 0.25$ and the parameters of explicit region $\gamma^E = 0.5$ and $\beta^E = 0$. The explicit-implicit asynchronous algorithm is used to solve the same model under the conditions of different time step ratios m .

5.1 Case of a cantilever beam in bending

A cantilever beam with rectangle section is presented. A bending load is subjected to the free end point A. The load time curve is shown in Fig. 5. The geometry and finite element mesh are shown in Fig. 6. The maximum force is 10000 N.

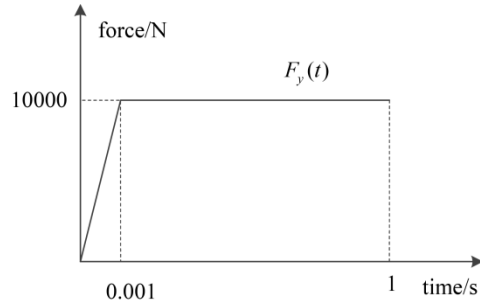


Figure 5: The load time curve for cantilever beam

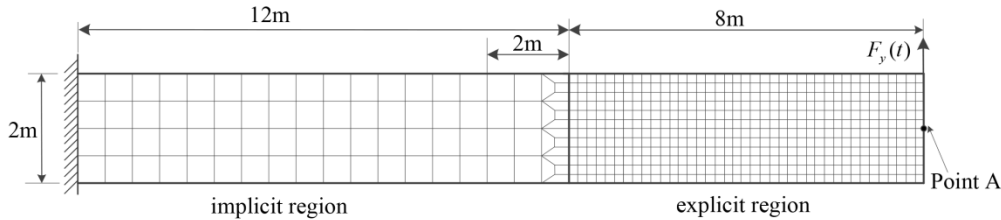


Figure 6: The geometry and finite element mesh of cantilever beam

The thickness of the rectangular cross-section is 0.03 m. The material is isotropic, linear elastic with Young's modulus $E=210 \times 10^9$ Pa, mass density $\rho=7800$ kgm⁻³ and Poisson ratio $\nu=0.3$. The beam is discretized into isoparametric quadrilateral element. The mesh size of the element in the coarse grid region is about 3 times of the size in the fined area. The whole element number of the region is 1080.

The step of the explicit region is defined by the CFL condition: $\Delta t_{cr}=5.78 \times 10^{-5}$ s. In this case, we use the step $\Delta t_r=5 \times 10^{-5}$ s for explicit region. The implicit region adopts a large time step Δt .

Under the condition of time step ratio $\Delta t=6\Delta t_r$, vertical displacement of point A is compared with the classical mixed method [Wu and Smolinski (2000)]. The vertical displacements of point A are shown in Fig. 7.

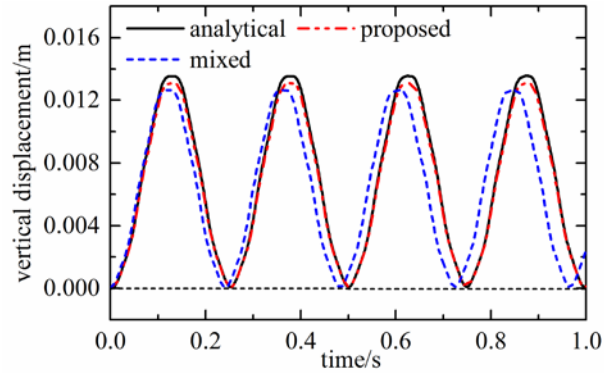


Figure 7: The vertical displacements of point A for different methods

Then we compare the accuracy of the algorithm under three different time step ratios $m=3$, $m=12$ and $m=24$. Fig. 8 compares the vertical displacement of point A. Fig. 9 is the local enlarged of Fig. 8. It can be find that the displacement curve is basically coincident and the accuracy of the algorithm is not significantly decreased with the step ratio increase.

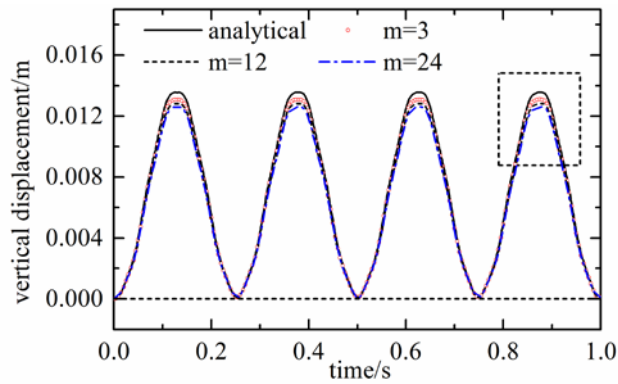


Figure 8: The vertical displacements of point A for different step ratios

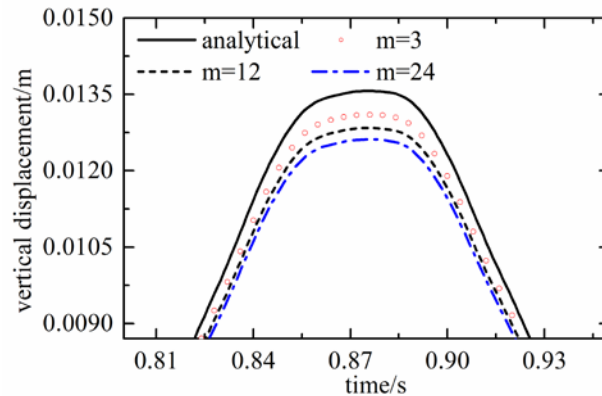


Figure 9: Local enlarged of Fig. 8

In order to analyze quantitatively the computational accuracy, we define sum of displacement errors u_{err} and maximum error of displacement u_{max} two indexes as

$$u_{err} = \|\mathbf{u}_{prop} - \mathbf{u}_{the}\|_2; u_{max} = \left| \mathbf{u}_{prop}^i - \mathbf{u}_{the}^i \right|_{\max} \quad (22)$$

Where \mathbf{u}_{the} means the theoretical displacement, \mathbf{u}_{prop} means the displacement calculated by different method and i is time step. The displacement error for different methods are counted as shown in Tab. 1. Although with the increase of the step ratio m , the two precision indexes is increasing for both methods. The interpolation process of boundary data is not involved in the proposed method and it has higher computational accuracy than traditional mixed explicit implicit method.

Table 1: Sum of displacement error u_{err} and maximum error of displacement u_{max} for different methods and step ratios m

Step ratio	Proposed method		Mixed method	
	u_{err}	$u_{max}(10^{-4})$	u_{err}	$u_{max}(10^{-4})$
$m=3$	0.237	2.03	0.952	6.27
$m=6$	0.413	5.84	2.208	10.25
$m=12$	0.608	7.31	3.986	13.64
$m=24$	0.845	10.80	6.197	17.15

The energy curve Fig. 10 shows that the dissipation energy almost zero for step ratio $m=12$. Namely, the development of pseudo energy does not appear in the computational process. The method is stability for a larger step ratio condition.

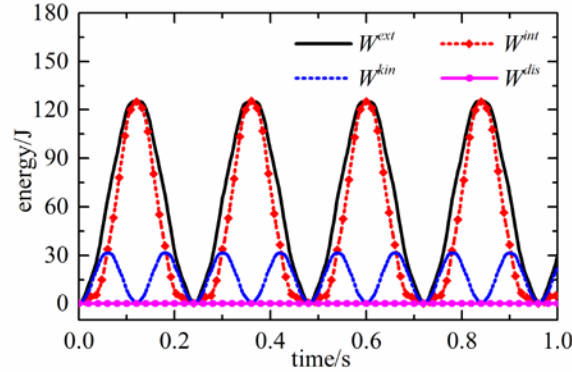


Figure 10: The energy curve of cantilever beam with step ratio $m=12$

The computation time for different methods is counted as shown in Tab. 2.

The two methods can reduce the calculation time. But the traditional mixed method needs to solve the global stiffness matrix at system time level. This has caused an increase in computing time to a certain extent. The proposed multiple partition boundary method can also reduce the computational time while maintain a higher accuracy.

Table 2: Computation time for cantilever beam with different methods and different step ratio m ; Step for explicit region and benchmark implicit method are $\Delta t_r=1\times 10^{-5}$ s

Solve method	Step ratio	Computation time/s	Percentage
Implicit method		315.2	100.0%
Mixed method	$m=3$	255.5	81.06%
	$m=6$	226.4	71.83%
	$m=12$	201.9	64.04%
	$m=24$	165.7	52.57%
Proposed method	$m=3$	187.4	59.45%
	$m=6$	161.3	51.17%
	$m=12$	138.0	43.78%
	$m=24$	110.9	35.21%

5.2 Case of a building in exploding

This case considers the dynamic response of a building under the explosion shock wave. The shock wave pressure, the overpressure peak value, impulse and duration are used to describe the explosion shock wave. The explosion shock can be simplified as a right triangle pulse load on the front of the structure, retaining its peak and duration characteristics [Ngo, Mendis, Gupta et al. (2007)].

The blasting shock wave conditions are set as showed in Tab. 3. The external force is loaded in the form of equivalent nodal load. The damping ratio of the structure is 5%, which load in the form of Rayleigh damping. The parameters of concrete are taken as follows: Mass density $\rho=2500 \text{ kgm}^{-3}$, the material Young modulus $E=30 \text{ GPa}$ and Poisson ratio $\nu=0.2$. The model is discretized into three dimensional hexahedral linear fully integrated elements. The mesh number of the model is 144384. There are 21657 elements in explicit region. The critical time step of explicit region is $\Delta t_{cr}=1.43\times 10^{-4}$ s. The time step $\Delta t_r=1.15\times 10^{-4}$ s is adopted in this case.

Table 3: Blast load considered in dynamic analysis

Load case	Explosive mass /kg	Distance /m	Reflected overpressure /kPa	Impulse /kPa·ms	Positive phase duration/ms
1	100	10	846	1543	9.7
2	200	10	1699	2582	12.1
3	500	10	4250	5172	17.5
4	500	15	1254	3096	16.2
5	500	20	535	2186	18.4

Explicit-implicit asynchronous time step algorithm is used to solve the whole finite element simulation model and the explicit-implicit partition is shown in Fig. 11.

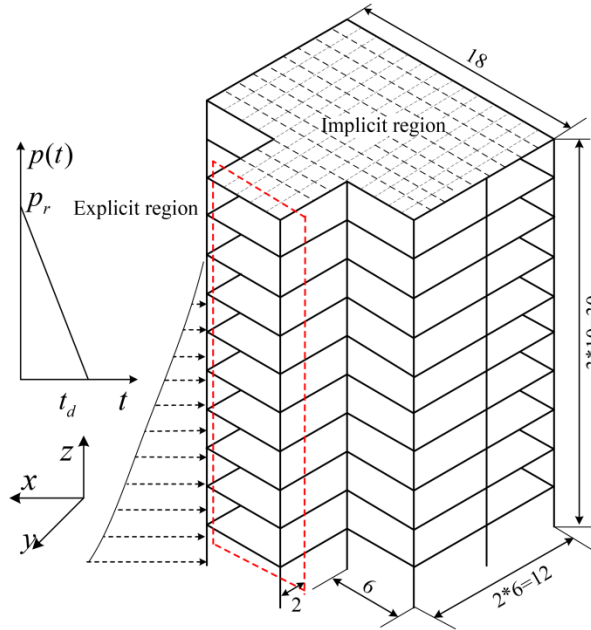


Figure 11: A building model under explosion shock wave

For the response of building structure under earthquake or other impacts, the inter layer displacement angle is an important parameter. Fig. 12 compares the distribution of the maximum inter layer displacement angle of the building structure under five loading conditions [Jayasooriya, Thambiratnam, Perera et al. (2011)]. We choose the step ratio $m=3$, which means the time step $\Delta t=3\Delta t_r$ is used in the implicit region.

The results of Fig. 12 show that the response of the building structure is influenced significantly by the mass of the explosive and the distance of the explosion point. When the 2 and 4 of the working conditions, the maximum inter story drifts angle of the structure is close to 4%. And the structural deformation under the load condition 3 is much larger than that of the other working conditions. The maximum lateral drift of the building is more than 10%, which will produce great damage to the building.

Fig. 13 compares the inter layer displacement angle of three different step ratios m at the same load case 2. With the increase of the step ratio m , the three calculation results have the same change rule.

Fig. 14 is the displacement time curve at the top of the building in the direction of the impact of the shock wave. At the same load case 2, displacement time curve of the explicit method, the proposed method and the classical mixed method (reference method) are compared [Wu and Smolinski (2000)]. The maximum displacement reaches 124 millimeters. It is necessary to further analyze the displacement response of the building under various load conditions.

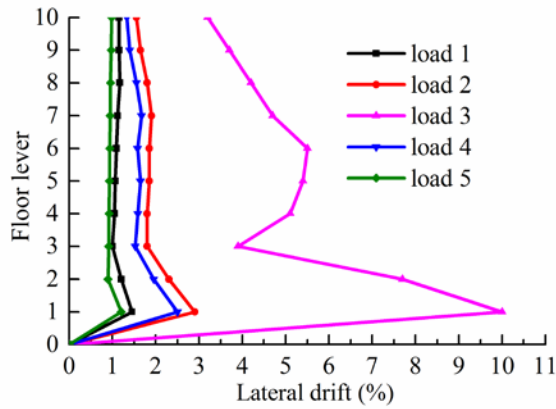


Figure 12: The maximum inter layer displacement angle of the building

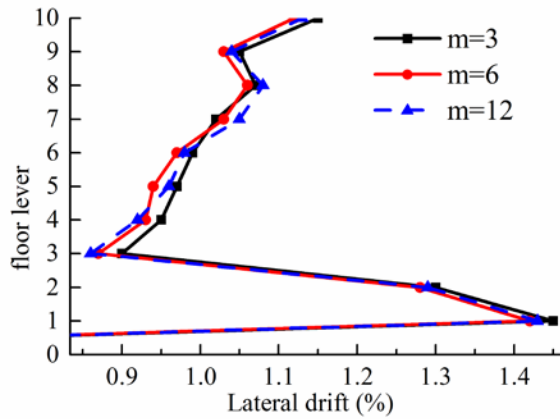


Figure 13: The inter layer displacement angle of different step ratios m under load case 2

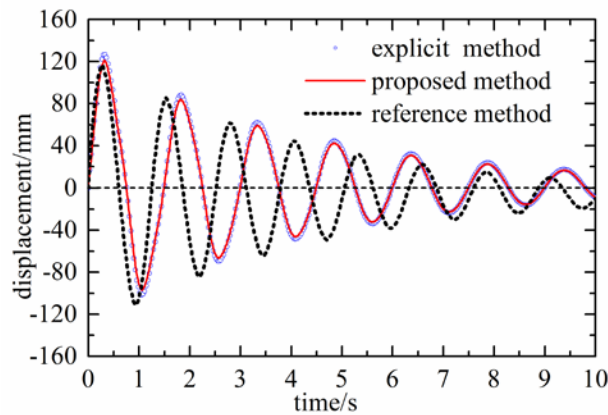


Figure 14: The displacement time curve at the top of the building

The computational efficiency of traditional central difference algorithm and the proposed algorithm are compared in this paper. The CPU time is calculated by the different

selected step ratios m . The computation time consumed for different methods is shown in Tab. 4.

Table 4: Computation time for a building in exploding with different methods and different step ratio m ; time step $\Delta t=1.15 \times 10^{-4}$ s for explicit region and benchmark explicit method

Solve method	Step ratio	Computation time/s	Percentage
Explicit method		10324	100.0%
Mixed method	$m=1$	8538	82.7%
	$m=3$	7165	69.4%
	$m=10$	6053	58.6%
	$m=30$	4656	45.1%
Proposed method	$m=1$	6927	67.1%
	$m=3$	5430	52.6%
	$m=10$	4037	39.1%
	$m=30$	2911	28.2%

The computation time required for solving the same physical problem is greatly reduced by using the multi-scale discrete grid and the different step size in the time domain. The more nodes are used in large step size, the greater computational efficiency is obtained. The proposed method has the potential for practical application in large scale computation.

6 Conclusions

In many actual dynamic engineering applications, the system has different physical and mechanical properties. The accuracy requirement of the different parts of the system determines the scale of the finite element discrete mesh, which limits the time step.

In this paper, an explicit-implicit multi-time-step method of finite element is proposed to solve this problem. Compared with other time integration analysis methods, this method has several characteristics:

- (1) According to the mechanical properties and computational accuracy of a different computing domain, in both space and time domain, the model is simulated with different scales. The more nodes are used in large step size, the greater computational efficiency of the theory can be obtained.
- (2) The algorithm uses the changing boundary nodes to deal with the coupling between large and small steps. There is no additional assumption on the boundary node information transfer. The larger time step ratio can be used in theory.
- (3) The energy balance method can be used to find the generation of pseudo-energy and unstable development in calculation. It is helpful to get more reasonable calculation results in real time to adjust the calculation step.

To a certain extent, the changing boundary nodes method increases the difficulty of pre-processing. If the algorithm can be reasonably parallel and the calculation domain is optimized to achieve load balance, the method must be able to obtain a good performance in solving the super large scale application. It will be the focus of further research.

Acknowledgement: The project is supported by the National Key Research and Development Program of China (2016YFB0201800) and the National Natural Science Foundation of China (No. 51475287 and No. 11772192).

References

- Belytschko, T.; Mullen, R.** (1978): Stability of explicit-implicit mesh partitions in time integration. *International Journal for Numerical Methods in Engineering*, vol. 12, no. 10, pp. 1575-1586.
- Biesiadecki, J. J.; Skeel, R. D.** (1993): Dangers of multiple time step methods. *Journal of Computational Physics*, vol. 109, no. 2, pp. 318-328.
- Bock, H. G.; Kirches, C.; Meyer, A.; Potschka, A.** (2018): Numerical solution of optimal control problems with explicit and implicit switches. *Optimization Methods and Software*, vol. 33, no. 3, pp. 450-474.
- Chen, J.; Wang, J.** (2016): Three-dimensional dispersive hybrid implicit-explicit finite-difference time-domain method for simulations of graphene. *Computer Physics Communications*, vol. 207, pp. 211-216.
- Combescure, A.; Gravouil, A.** (2002): A numerical scheme to couple subdomains with different time-steps for predominantly linear transient analysis. *Computer Methods in Applied Mechanics and Engineering*, vol. 191, no. 11, pp. 1129-1157.
- Cook, R. D.** (2007): *Concepts and Applications of Finite Element Analysis*. John Wiley & Sons.
- Daniel, W. J. T.** (2003): A partial velocity approach to subcycling structural dynamics. *Computer Methods in Applied Mechanics and Engineering*, vol. 192, no. 3, pp. 375-394.
- Dimarco, G.; Pareschi, L.** (2017): Implicit-explicit linear multistep methods for stiff kinetic equations. *SIAM Journal on Numerical Analysis*, vol. 55, no. 2, pp. 664-690.
- Fekak, F. E.; Brun, M.; Gravouil, A.; Depale, B.** (2017): A new heterogeneous asynchronous explicit-implicit time integrator for nonsmooth dynamics. *Computational Mechanics*, vol. 60, no. 1, pp. 1-21.
- Fernandes, M. T. C. A.; Cardoso, C. O.; Mansur, W. J.** (2017): An adaptive load stepping algorithm for path-dependent problems based on estimated convergence rates. *Computer Modeling in Engineering & Sciences*, vol. 113, no. 3, pp. 325-342.
- Ghanem, A.; Torkhani, M.; Mahjoubi, N.; Baranger, T. N.; Combescure, A.** (2013): Arlequin framework for multi-model, multi-time scale and heterogeneous time integrators for structural transient dynamics. *Computer Methods in Applied Mechanics & Engineering*, vol. 254, pp. 292-308.
- Hughes, T. J. R.; Liu, W. K.** (1978): Implicit-explicit finite elements in transient analysis: Stability theory. *Journal of applied Mechanics*, vol. 45, no. 2, pp. 371-374.

- Hughes, T. J. R.** (2012): *The Finite Element Method: Linear Static and Dynamic Finite Element Analysis*. Courier Corporation.
- Jayasooriya, R.; Thambiratnam, D. P.; Perera, N. J.; Kosse, V.** (2011): Blast and residual capacity analysis of reinforced concrete framed buildings. *Engineering Structures*, vol. 33, no. 12, pp. 3483-3495.
- Jung, D. W.; Yang, D. Y.** (1998): Step-wise combined implicit-explicit finite element simulation of autobody stamping processes. *Journal of Materials Processing Technology*, vol. 83, no. 1, pp. 245-260.
- Karimi, S.; Nakshatrala, K. B.** (2014): On multi-time-step monolithic coupling algorithms for elastodynamics. *Journal of Computational Physics*, vol. 273, pp. 671-705.
- Krenk, S.** (2006): Energy conservation in newmark based time integration algorithms. *Computer Methods in Applied Mechanics and Engineering*, vol. 195, no. 44, pp. 6110-6124.
- Liu, W. K.; Belytschko, T.** (1982): Mixed-time implicit-explicit finite elements for transient analysis. *Computers & Structures*, vol. 15, no. 4, pp. 445-450.
- Mahjoubi, N.; Gravouil, A.; Combescure, A.** (2009): Coupling subdomains with heterogeneous time integrators and incompatible time steps. *Computational Mechanics*, vol. 44, no. 6, pp. 825-843.
- Narasimhan, N.; Lovell, M.** (1999): Predicting springback in sheet metal forming: An explicit to implicit sequential solution procedure. *Finite Elements in Analysis and Design*, vol. 33, no. 1, pp. 29-42.
- Ngo, T.; Mendis, P.; Gupta, A.; Ramsay, J.** (2007): Blast loading and blast effects on structures-an overview. *Electronic Journal of Structural Engineering*, vol. 7, pp. 76-91.
- Noels, L.; Stainier, L.; Ponthot, J. P.** (2004): Combined implicit-explicit algorithms for crashworthiness analysis. *International Journal of Impact Engineering*, vol. 30, no. 8, pp. 1161-1177.
- Noels, L.; Stainier, L.; Ponthot, J. P.** (2006): Energy conserving balance of explicit time steps to combine implicit and explicit algorithms in structural dynamics. *Computer Methods in Applied Mechanics and Engineering*, vol. 195, no. 19, pp. 2169-2192.
- Prakash, A.; Hjelmstad, K. D.** (2004): A FETI-based multi-time-step coupling method for Newmark schemes in structural dynamics. *International Journal for Numerical Methods in Engineering*, vol. 61, no. 13, pp. 2183-2204.
- Smolinski, P.; Belytschko, T.; Neal, M.** (1988): Multi-time-step integration using nodal partitioning. *International Journal for Numerical Methods in Engineering*, vol. 26, no. 2, pp. 349-359.
- Soares, D.** (2018): Nonlinear dynamic analysis considering explicit and implicit time marching techniques with adaptive time integration parameters. *Acta Mechanica*, vol. 229, no. 3, pp. 2097-2116.
- Wu, Y. S.; Smolinski, P.** (2000): A multi-time step integration algorithm for structural dynamics based on the modified trapezoidal rule. *Computer Methods in Applied Mechanics and Engineering*, vol. 187, no. 3, pp. 641-660.